Shear-induced discontinuous and continuous topological transitions in a hyperswollen membrane system

Hajime Tanaka,* Mamoru Isobe,† and Hideyuki Miyazawa‡
Institute of Industrial Science, University of Tokyo, Meguro-ku, Tokyo 153-8505, Japan
(Received 24 June 2005; revised manuscript received 4 November 2005; published 7 February 2006)

Here we demonstrate that both discontinuous and continuous transition between the sponge and lamellar phase can be induced by steady shear flow for a hyperswollen membrane system. The discontinuous nature of the transition is revealed by a distinct hysteresis in the rheological behavior between shear-rate increasing and decreasing measurements at a constant temperature. This discontinuity becomes weaker with an increase in the shear rate and temperature, and the transition eventually becomes a *continuous* one without any hysteresis. We also found another shear-induced transition in a one-phase lamellar region. The dynamic phase diagram in a nonequilibrium steady state under shear is constructed for the sponge-lamellar transition as well as another transition in a stable lamellar phase. Possible physical mechanisms for these shear-induced transitions are discussed.

DOI: 10.1103/PhysRevE.73.021503 PACS number(s): 83.80.Qr, 82.70.Uv, 61.30.St, 83.60.Rs

I. INTRODUCTION

Shear-induced phase transformation have recently attracted much attention from both fundamental and industrial viewpoints [1]. Since the transition occurs between nonequilibrium steady states, kinetic effects associated with energy dissipation, such as hydrodynamic and viscoelastic effects, play key roles in the transformation, unlike the equilibrium phenomena. Because of this fundamental difficulty, the nature of such a transition and the principle of phase selection (or, more strictly, state selection) remains an open problem of nonequilibrium soft matter physics.

One of the important issues associated with this problem is the coupling between shear flow and an internal structure of complex fluids, which controls the rheological properties. In particular, bilayer membranes can be organized with various topologies, such as sponge, lamella, and onions; thus, the coupling between the shear field and the membrane organization is of great interest. Two types of shear-induced transitions have been well known: (i) lamellar-to-onion and (ii) sponge-to-lamellar transition. The former was found by Diat and Roux [2]. Since then, there have been intensive studies on the instability of a lamellar phase under shear and the formation of the so-called onions both experimentally [3–9] and theoretically [10–14]. This transition exhibits extremely rich behavior and the physical mechanism has still not been fully clarified yet.

Among various kinds of shear effects on complex fluids, shear effects on an isotropic-smectic transition are interesting in relation to two types of fluctuation effects. One is the fluctuation associated with the Landau-Peierls instability intrinsic to low-dimensional systems. This results in the *coherent* undulation fluctuations of the smectic order, whose amplitude logarithmically diverges with an increase in the system size. The other is the Brazovskii-type fluctuation effect [15], which is associated with the selection of the orientation of the smectic order from a highly symmetric isotropic phase. This is responsible for the so-called fluctuation-induced first-order transition in this type of system [10]. The isotropic-smectic transition is generic to (a) thermotropic liquid crystals [16], (b) block copolymers (isotropic-lamellar transition) [17], and (c) lyotropic liquid crystals (sponge-lamellar transition) [18–22] reflecting the common nature of the change in the structural symmetry.

Here we focus on shear effects on a sponge-to-lamellar transition in system (c), which is observed in aqueous solutions of bilayer-forming amphiphiles. In addition to the above-mentioned universal features associated with the symmetry of the system, this transition has unique features, which are absent in the other two systems (a) and (b): (i) It is a two-component system, which is composed of membranes and intermembrane fluids. (ii) The corresponding isotropic phase (L_3 phase, or "sponge phase") has an internal structure of interconnected membranes [23,24]. Since both phases are constructed by the same bilayers, they can be distinguished only by the topology of membranes. (iii) The lamellar phase is stabilized by entropic repulsion between fluctuating membranes, which is known as "Helfrich interaction." These *incoherent* fluctuations of membranes are directly affected by shear flow, which affects the intermembrane interaction itself [14,25,26].

Shear effects on a sponge-lamellar transition have been studied by a few groups, but the conclusions derived from these studies are sometimes even controversial [27]. The most fundamental issue remaining is whether the transition is discontinuous or continuous [20,21]. We previously demonstrated the transition changes from a discontinuous to a continuous one while increasing the shear rate *for oscillatory shear* [19]. Leon *et al.* [20] found the discontinuous nucleation of the lamellar phase in the sponge phase *under steady*

*Electronic address: tanaka@iis.u-tokyo.ac.jp
†Present address: Technology & Product Development Division, OPTREX, Arakawa-ku, Tokyo 116-0014, Japan.
‡Present address: Core Technology Research Center, Research and Development Group, RICOH Company, Ltd., Atsugi, Kanagawa 243-0298, Japan.

 ©2006 The American Physical Society

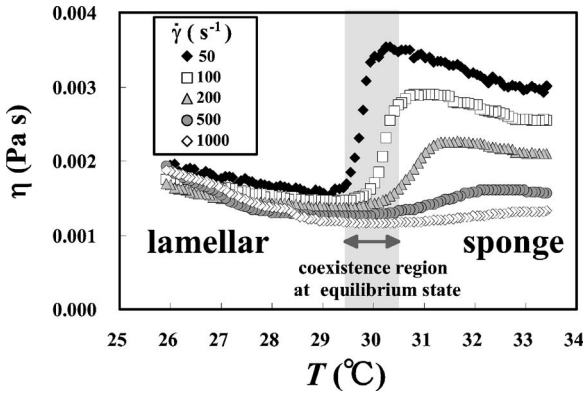

FIG. 1. Temperature dependence of the viscosity across the transition from the sponge to the lamellar phase under a constant shear rate upon cooling.

shear and revealed the importance of the delayed transition associated with the metastability of the phenomena. Porcar *et al.* [21], on the other hand, concluded that the transition is always continuous *under steady shear*. According to the Cates-Milner theory [10], the transition is of first-order nature and there is no distinct discontinuous-continuous transition; the discontinuous nature continuously weakens with an increase in the shear rate. Thus, there have so far been no coherent view on this problem. In this paper, we study this problem to improve the above confusing situation. We also report another shear-induced transition found in the one-phase lamellar phase.

The organization of our paper is as follows. In Sec. II, we describe the details of our experiments. In Sec. III, we describe the experimental results on two types of shear-induced transitions and discuss the physical mechanisms. In Sec. IV, we summarize our work.

II. EXPERIMENTAL

The lyotropic liquid crystal system studied here is a two-component mixture of triethylenglychol mono-*n*-decyl ether ($C_{10}E_3$) and water [7]. We mainly used the 1.39 wt. % $C_{10}E_3$ solution, which forms a hyperswollen sponge and a lamellar phase. With an increase in the temperature T, the system

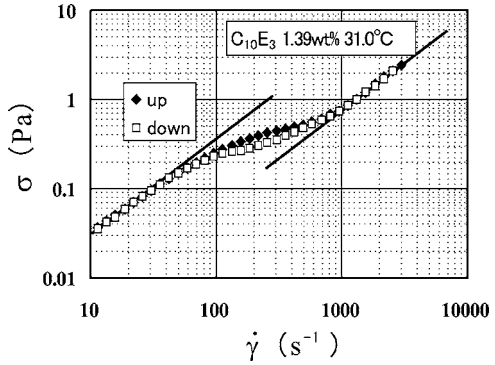

FIG. 2. σ-$\dot{\gamma}$ relationship measured at $T=31$ °C. A clear hysteresis can be seen between the shear-rate increasing (filled diamonds) and decreasing (open squares) run. The slope of the lines are 1.

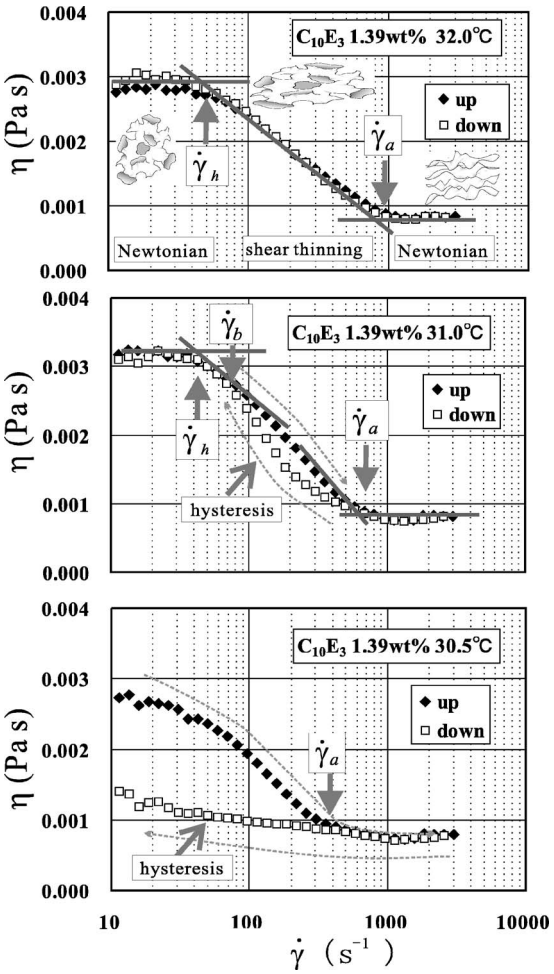

FIG. 3. Shear-rate dependences of the effective viscosity ($\eta = \sigma/\dot{\gamma}$) for $C_{10}E_3$/water (1.39 wt. % $C_{10}E_3$) at 32.0 °C (top), 31.0 °C (middle), and 30.5 °C (bottom). η was measured for both increasing (filled symbols) and decreasing the shear rate (open symbols). There was no hysteresis at 32.0 °C, whereas there was a clear one at 31.0 °C and 30.5 °C. This suggests the transition is continuous at 32.0 °C, but discontinuous at 31.0 °C and 30.5 °C. In the top figure, we put schematic drawings of isotropic and anisotropic sponge and lamellar structures.

changes from the lamellar (L_α) to the sponge-lamellar coexistence phase at $T_\alpha=29.5$ °C, and further from the coexistence phase to the sponge (L_3) phase at $T_3=30.5$ °C. The existence of the two-phase coexistence region between the sponge and lamellar phase indicates a weak first-order character of the thermodynamic transition. The rheological properties were measured by a rheometer (Rheologica, StressTech) with a cone-plate geometry (cone angle=1°). Evaporation of water was prevented by oil sealing. Two types of measurements were made: (i) Temperature dependence of the effective shear viscosity η under a constant shear rate. Here η is defined as $\sigma/\dot{\gamma}$, where σ is the measured stress and $\dot{\gamma}$ is the applied shear rate. The measurements were started in the sponge phase and the temperature was cooled with a cooling rate of 0.2 K/min. (ii) Shear-rate dependence of η at a constant temperature. Shear increasing and decreasing measurements are performed to study the

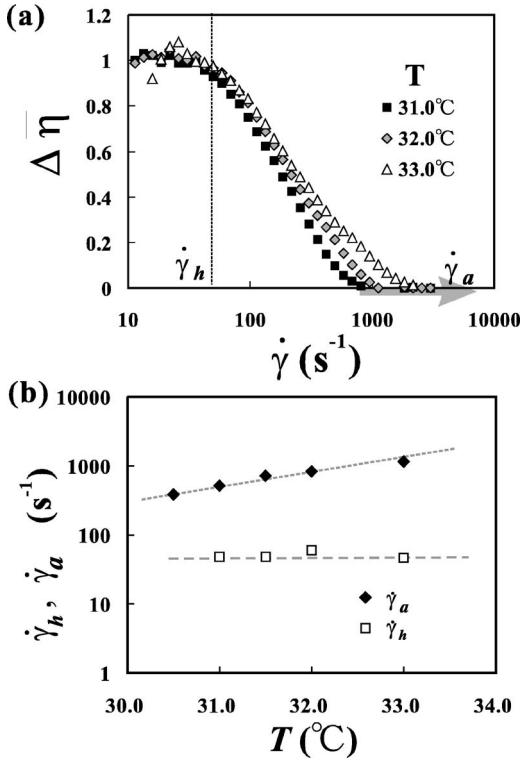

FIG. 4. (a) $\dot{\gamma}$ dependence of the normalized viscosity difference (see text for the definition). (b) T dependences of $\dot{\gamma}_h$ and $\dot{\gamma}_a$.

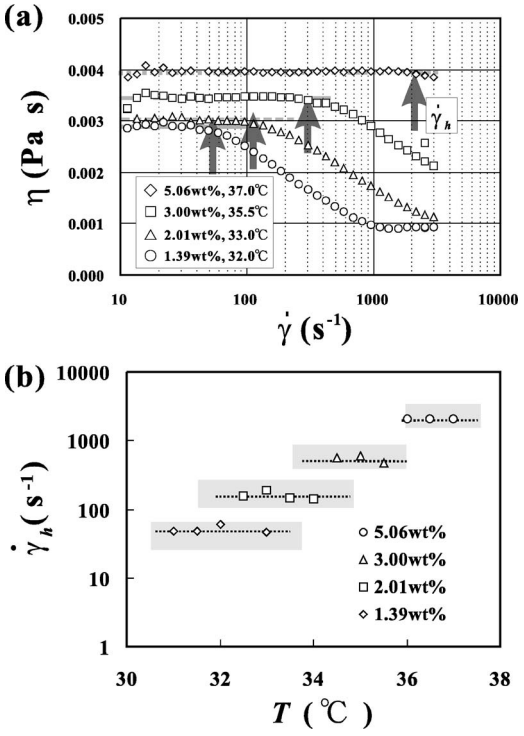

FIG. 5. (a) ϕ dependence of the shear-thinning behavior of the sponge phase. The location of $\dot{\gamma}_h$ is indicated by an arrow for each composition. (b) Dependences of $\dot{\gamma}_h$ on T and ϕ. $\dot{\gamma}_h$ is independent of T, but increases with ϕ.

hysteresis effect. The shear rate was scanned between 10 s^{-1} and 3000 s^{-1} during 20–60 min. We confirmed that the scan rate does not affect the results in this range of $d\dot{\gamma}/dt$. Dynamic light scattering measurements were performed by using a correlator (ALV, ALV-5000/E).

III. RESULTS AND DISCUSSION

A. Shear-induced sponge-lamellar transition

1. Rheological properties

Figure 1 shows the results of the temperature dependence of η of the 1.39 wt. % $C_{10}E_3$ aqueous solution for several shear rates. For a low shear rate, a distinct steplike decrease of η upon cooling is clearly observed. However, this discontinuous nature becomes weaker with an increase in the shear rate $\dot{\gamma}$ and eventually the transition apparently becomes continuous at $\dot{\gamma}=1000$ s^{-1}. It is known that the viscosity of the sponge phase is a few times higher than that of the lamellar phase [25,28]. This high viscosity of the sponge phase is due to the fact that the passage of the membrane disturbs shear flow fields. On the contrary, there is likely little disturbance to shear flow fields in the lamellar phase. This fact can be a primary cause of shear-induced sponge-to-lamellar transition; the state may be selected so as to decrease the viscous dissipation.

Figure 2 indicates the stress (σ)-strain rate ($\dot{\gamma}$) curve measured for $T=31$ °C. Although there is no plateau in the σ-$\dot{\gamma}$ curve, there is a clear hysteresis between the shear-rate increasing and decreasing measurement. To see the hysteresis effects more clearly, in Fig. 3 we show the results of the shear-rate dependence of $\eta(=\sigma/\dot{\gamma})$ for $T=32$ °C, 31 °C, and 30.5 °C. For both low and high shear rates, the system exhibits Newtonian behavior (i.e., η is independent of $\dot{\gamma}$), while between $\dot{\gamma}_h$ and $\dot{\gamma}_a$ it exhibits strong shear-thinning behavior. There is no hysteresis at $T=32$ °C between increasing and decreasing $\dot{\gamma}$, whereas there is a clear hysteresis for $T=31$ °C and 30.5 °C. The upper bound of the hysteresis region coincides with $\dot{\gamma}_a$, at which the shear thinning starts to occur while increasing $\dot{\gamma}$. On the other hand, the lower bound $\dot{\gamma}_b$ is located above $\dot{\gamma}_h$. Note that at $T=30.5$ °C the system at rest is in the coexistence region of the sponge and lamellar phases. Reflecting this fact, there is no Newtonian regime at low shear rates at this temperature. It should be noted that although $\dot{\gamma}_h$ is independent of T, $\dot{\gamma}_a$ steeply increases with an increase in T.

Next we show how the critical shear rates $\dot{\gamma}_h$ and $\dot{\gamma}_a$ depend upon T. Figure 4(a) shows the $\dot{\gamma}$ dependence of the normalized viscosity difference $\Delta\bar{\eta}$, which is defined as $\Delta\bar{\eta}=[\eta(0)-\eta(\dot{\gamma})]/[\eta(0)-\eta(\dot{\gamma}>\dot{\gamma}_a)]$. The T dependences of $\dot{\gamma}_h$ and $\dot{\gamma}_a$ are also shown in Fig. 4(b). This clearly indicates that $\dot{\gamma}_h$, which is the onset of the shear thinning, is independent of T, whereas $\dot{\gamma}_a$, above which the system transforms into the homogeneous lamellar phase, increases with an increase in T.

Here we show the ϕ dependence of the shear-thinning behavior of the sponge phase in Fig. 5(a). $\dot{\gamma}_h$, where shear thinning starts while increasing $\dot{\gamma}$, increases with an increase in ϕ, which can be clearly seen in Fig. 5(b).

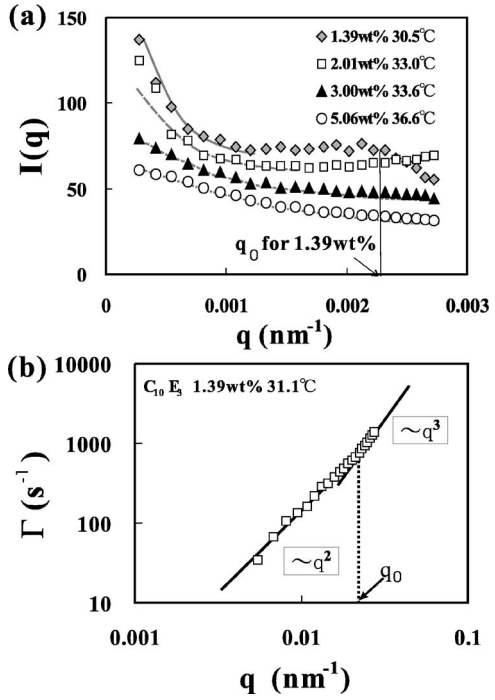

FIG. 6. (a) q dependence of the scattering intensity $I(q)$ for solutions of various ϕ's. (b) q dependence of the decay rate Γ for a solution of $\phi=1.39$ wt. %.

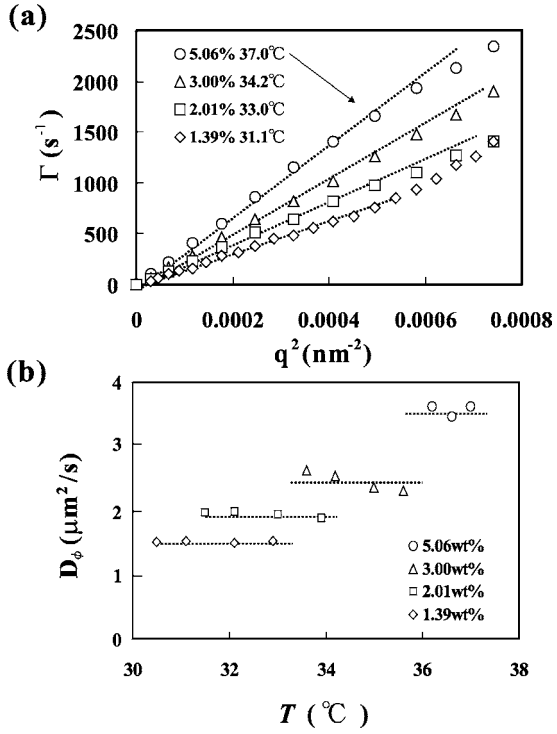

FIG. 7. (a) q dependence of the decay rate Γ for solutions of various ϕ's. (b) T dependence of D_ϕ for various ϕ's.

2. Dynamics of topological transformation in the equilibrium sponge phase: light-scattering study

The above results suggest that there is a characteristic time scale of topological transformation, which spontaneously takes place in the equilibrium sponge phase and is coupled with shear flow. To reveal the dynamics of the topological fluctuations, we performed light scattering measurements.

Figure 6(a) shows the static scattering intensity $I(q)$ as a function of the wave number q. Only for a solution of $\phi=1.39$ wt. %, we can see a peak at q_0, reflecting the pore size of the sponge phase. Note that $q_0=2\pi/d$ (d: average intermembrane distance or pore size). The intensity at $q\rightarrow 0$ grows in proportional to ϕ^{-1} [30].

We also performed dynamic light scattering experiments. The time correlation function is described by the stretched exponential function with the exponent of 0.7, which is consistent with the theoretical prediction of Zilman and Granek [33]. Figure 6(b) shows the q dependence of the decay rate Γ for a solution of $\phi=1.39$ wt. %. The q dependence changes at q_0 from $\Gamma\propto q^2$ to $\Gamma\propto q^3$, although the range of q seems to be too narrow for a conclusive argument. Figure 7(a) shows q dependence of the decay rate Γ for solutions of various ϕ's. Thus we confirm the diffusive nature of the mode from the q^2 dependence of the relaxation rate in the wave number range $q<q_0$. From the diffusive regime, we can determine the cooperative diffusion constant of membranes D_ϕ. The T dependence of D_ϕ is plotted for various ϕ's in Fig. 7(b).

3. Nature and mechanism of shear-induced sponge-lamellar transition

Let us consider the physical meanings of the key shear rates, $\dot{\gamma}_h$, $\dot{\gamma}_a$, and $\dot{\gamma}_b$, for the shear-induced sponge-lamellar transition. Both sponge and lamellar phases are constructed by the same membranes and their structures are not permanent but dynamically fluctuating. Thus, they can be easily reconstructed even by a weak perturbation [29–31]. In the sponge phase, shear flow tears off selectively the passages of the membrane that are not along the flow direction, if it is strong enough [29–31]; the sponge phase starts to become *anisotropic* if $\dot{\gamma}$ exceeds the characteristic rate of membrane reorganization (or reconnection) $\dot{\gamma}_h$. This rate $\dot{\gamma}_h$ can be estimated as [29,32]

$$\dot{\gamma}_h \sim \Gamma_D \exp(-\Delta E_A/k_BT), \tag{1}$$

using the characteristic frequency of membrane collisions, Γ_D, and the energy barrier for membrane reconnection, E_A. Here Γ_D can be estimated as $\Gamma_D\sim D_\phi q_0^2$.

The ϕ dependences of Γ_D and $\dot{\gamma}_h$ are plotted in Fig. 8. Both are found to be proportional to ϕ^3 (note that $\Gamma_D\propto\phi^3$ is the natural consequence of $D_\phi\propto\phi$ and $q_0\propto\phi$ [30]), in accord with the above argument. They are independent of T in the rather narrow temperature range of the sponge phase. From the ratio of $\dot{\gamma}_h/\Gamma_D$, we estimated E_A as $1.3k_BT$. Now it is clear that $\dot{\gamma}_h$ is the critical shear rate, above which $\dot{\gamma}$ exceeds the characteristic frequency of the topological transformation of membranes $\dot{\gamma}_h$. From this analysis, we can conclude that above $\dot{\gamma}_h$ the isotropic sponge becomes the anisotropic one, which should result in the appearance of optical birefringence [29]. This behavior can be viewed as the selection of the fluctuation modes by shear flow due to its symmetry-breaking nature.

Next we consider the physical meanings of $\dot{\gamma}_a$ and $\dot{\gamma}_b$. $\dot{\gamma}_a$ can be regarded as the crossover shear rate from the aniso-

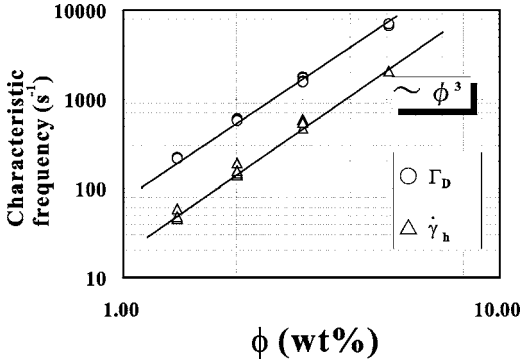

FIG. 8. ϕ dependence of $\dot{\gamma}_h$ and Γ_D. The slope of the lines are 3.0. At each concentration, we made measurements of $\dot{\gamma}_h$ and Γ_D at four different temperatures within a temperature range of the sponge phase (see Figs. 5 and 7). There were almost no temperature dependences, which can be confirmed by the fact that the symbols for the same ϕ are almost overlapped with each other.

tropic sponge to the lamellar phase. With an increase in $\dot{\gamma}$, shear flow breaks up more handles of the sponge structure that are not along the flow direction; thus, the sponge becomes more anisotropic, which leads to the shear thinning upon increasing $\dot{\gamma}$. This shear thinning is a natural consequence of the decrease in the number density of handles with an increase in the shear rate, on noting that the handles are obstacles for flow. At $\dot{\gamma}_a$, shear flow erase all the passages or handles and the characteristic length becomes equal to that of the lamellar phase. Thus, the lamellar phase is formed and the shear-induced sponge-to-lamellar transition is completed at $\dot{\gamma}_a$. Above $\dot{\gamma}_a$, η becomes independent of $\dot{\gamma}$. Above 32 °C, there is no hysteresis upon a shear-rate change, which indicates that the transition is continuous there. Below 32 °C, on the other hand, there is a clear hysteresis between $\dot{\gamma}_b$ and $\dot{\gamma}_a$. This region is the coexistence region of the anisotropic sponge and lamellar phases; in other words, the number of handles becomes spatially inhomogeneous. We emphasize that the existence of the hysteresis (the discontinuous nature of the transition) for a low shear rate is a natural consequence of the first-order nature of the thermodynamic sponge-lamellar transition for $\dot{\gamma}=0$. Here we summarize the observed behavior in the two-dimensional (2D) dynamic phase diagram for the 1.39 wt. % $C_{10}E_3$ aqueous solution (see Fig. 9).

Our σ-$\dot{\gamma}$ curve do not have any plateau even for a discontinuous transition, contrary to a common picture anticipated from a shear-banding system. For example, Porcar *et al.* [21] concluded the continuous nature of the transition from the absence of the stress plateau. We speculate that the absence of the plateau may be due to the absence of the macroscopic shear banding, that is, due to the finite size of coexisting domains. The plateau in the stress-strain relation should be observed only when we have macroscopic phases separated by interfaces aligned along the walls [34]. The extremely small interface tension may be a cause of the absence of macroscopic shear banding; note that the interface tension scales as d^{-2}. Furthermore, the interface tension between the anisotropic sponge and lamellar phases should be extremely weak, due to the small difference in the smectic order parameter; the only difference between the two phases is the number density and the orientation of handles. We also confirm that the shear-rate dependence of η, or the stress-strain curve, is not sensitive to the scanning rate of the shear rate in the range between 10 s^{-1}/min and 100 s^{-1}/min. Our study implies that the shape of the stress-strain curve cannot always be used to determine whether the transition is continuous or discontinuous. The hysteresis effects may be used as a criterion for whether a shear-induced transition is continuous or discontinuous.

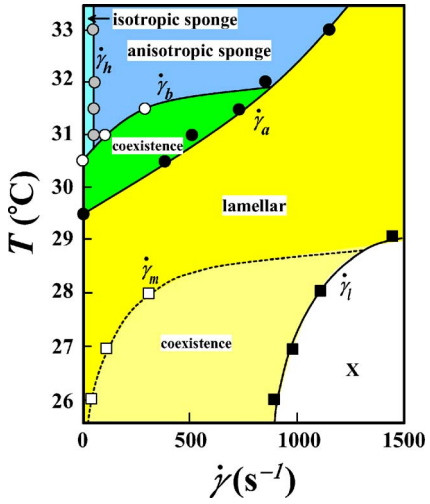

FIG. 9. (Color online) 2D dynamic phase diagram in the T-$\dot{\gamma}$ plane for $C_{10}E_3$/water (1.39 wt. % $C_{10}E_3$). X represents the unknown state, which might be an onion, a leek, an anisotropic micellar state, or a lamellar phase with a orientation.

Finally we mention that the strong temperature dependence of $\dot{\gamma}_a$ is suggestive of the strong temperature dependence of the thermodynamic factor of the sponge-lamellar transition. The most probable candidate is the Gaussian curvature modulus $\bar{\kappa}$. $\bar{\kappa}$ may change its sign from positive to negative upon cooling, reflecting the decrease of the conformational disorder of hydrophobic chains of the surfactant molecules and the resulting change in the spontaneous curvature of a monolayer membrane [35]. Thus, the temperature dependence of $\bar{\kappa}$ may be one of the main driving factors of the sponge-to-lamellar transition [7].

B. Shear-induced transition in the lamellar phase

Figures 10(a) and 10(b) show the $\dot{\gamma}$ dependence of η for $T=29.0$ °C and 27.0 °C, respectively. The lamellar phase exhibits shear-thinning behavior [25] up to $\dot{\gamma}_l$, but η slightly increases above $\dot{\gamma}_l$ (slight shear thickening). This trend can also be seen in Fig. 1. This might reflect the lamellar-onion transition, which was first reported by Le *et al.* [7] for the same system, but at a higher surfactant concentration. The hysteresis behavior is also observed for this transition between $\dot{\gamma}_m$ and $\dot{\gamma}_l$ below 29 °C. This transition is also revealed to be discontinuous at low temperatures, but at least *apparently* continuous at high temperatures. The lamellar phase that is stabilized by Helfrich repulsions becomes less stable under shear, since *incoherent* membrane fluctuations,

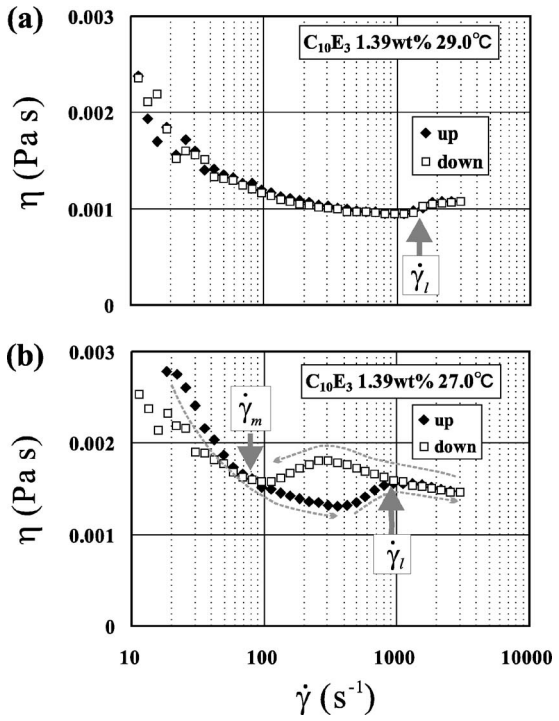

FIG. 10. Shear-rate dependences of the effective viscosity for $C_{10}E_3$/water (1.39 wt. % $C_{10}E_3$) at (a) 29.0 °C and (b) 27.0 °C. There was no hysteresis for (a), while there was a clear one for (b).

which is the origin of entropic repulsions, are suppressed by shear [11,12,14]. This was confirmed experimentally [25,36].

The temperature dependence of the stability limit $\dot{\gamma}_l$ is predicted theoretically as $\dot{\gamma}_l \propto T^{5/2}$ [11,14]. However, the temperature dependence is much stronger than this prediction, as shown in Fig. 9. The very strong temperature dependence of $\dot{\gamma}_l$ (also $\dot{\gamma}_a$) clearly indicates the importance of the thermodynamic factors of the underlying phase transitions, in particular, the role of the Gaussian curvature modulus $\bar{\kappa}$. In other words, the relevant variable may not be the absolute temperature T, but may be the temperature distance from some critical temperature. For this system, the sponge-lamellar and lamellar-onion transition may be induced by the change in the sign of $\bar{\kappa}$ from negative to positive upon cooling [7,14]. This change is induced by the decrease of the effective volume of a tail of a surfactant molecule upon cooling, reflecting the population of gauche and trans conformations of a tail. We point out a possibility that the lamellar phase may become a metastable frustrated state against the onion phase upon cooling.

At this moment, we cannot say anything conclusive on the nature of this transition observed in the lamellar phase. What we can say is that this transition is a consequence of the instability of the *c*-oriented lamellar phase induced by shear [11,12,14,25,36]. Here we just speculate about its nature from the limited information of our rheological measurements. The state "*X*" appearing at high $\dot{\gamma}$ might be an onion, a leek, or an anisotropic micellar phase, which is related to a lower-temperature phase existing below the one-phase lamellar phase. There is also a possibility that the transition reflects the change of the lamellar orientation. According to

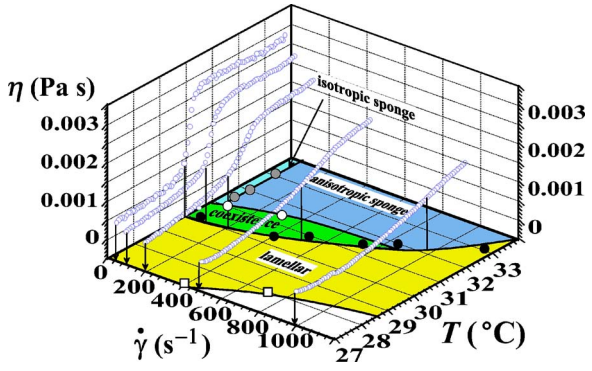

FIG. 11. (Color online) 3D dynamic phase diagram in the T-$\dot{\gamma}$-η space for $C_{10}E_3$/water (1.39 wt. % $C_{10}E_3$).

our previous study, membranes in the lamellar phase are oriented in perpendicular to the shear gradient direction (∇V) for a weak steady shear [25] and for an oscillatory shear [19]. The same conclusion was drawn by Porcar *et al.* for a steady shear flow [21]. This orientation is known as *c* orientation. This *c* orientation may transform into so-called *a* orientation, in which membranes in the lamellar phase is oriented in perpendicular to the vorticity direction. Here we note that in *c* orientation shear flow suppresses *incoherent* out-of-plane fluctuations of membranes, weakens the Helfrich repulsion, and thus destabilizes the lamellar phase, whereas in *a* orientation this effect may be absent. If this is the case, there is a coexistence of two types of orientation between $\dot{\gamma}_m$ and $\dot{\gamma}_l$. It seems to be a bit difficult to explain the strong T dependence of the critical shear rates in this mechanism. Finally, we point out that this phenomenon may be closely related to the shear-induced collapse of a lamellar phase recently reported by Porcar *et al.* [36]: They called the *X* state a collapsed state. They suggested that it might be an aligned tubular vesicle structure. This is certainly one possibility. Further studies are highly desirable for revealing the physical mechanism of this nonequilibrium phase transition. Scattering experiments [36] and measurements of flow birefringence may provide us with crucial information on the nature of the transition.

Finally, we summarize the observed behavior in three-dimensional (3D) dynamic phase diagrams for the 1.39 wt. % $C_{10}E_3$ aqueous solution in Fig. 11 together with the temperature dependence of viscosity.

IV. SUMMARY

In summary, we demonstrated that the shear-induced sponge-lamellar transition in a lyotropic liquid crystal changes its nature from discontinuous to continuous with an increase in the shear rate. The dynamic phase diagram in the T-$\dot{\gamma}$ plane for the nonequilibrium steady state is constructed; the basic feature of the sponge-lamellar transition under steady shear is essentially the same as that obtained for an oscillatory shear [19]. We speculate that this transition from discontinuous to continuous transformation with increasing the shear rate is a generic feature of the shear-induced sponge-lamellar transition. This point needs to be further studied both experimentally and theoretically in the future.

We also showed that the absence of the stress plateau in the stress-strain rate curve does not necessarily mean the continuous nature of the transition. The hysteresis of shear-rate increasing and decreasing experiments can be used as a fingerprint of the discontinuous nature of the transition.

The nature of the shear-induced transition found in the stable lamellar region is not clear now. This transition may be a result of the instability of the *c*-oriented lamellar phase induced by shear flow [11,12,14,25,36]. It might be the transformation of the lamellar phase into an onion, a leek, or an anisotropic micellar phase, or the orientational transition from so-called *c* to *a* orientation. It might be an aligned tubular vesicle structure, as suggested by Porcar *et al.* [36]. Among these possibilities, the continuous lamellar-to-onion transition seems to be difficult to accept due to their symmetries. The apparently continuous nature of this transition above 29 °C seems to imply some continuous pathway from a lamellar structure to an other unknown structure (a collapsed state) or a lamellar structure with a different orientation. The relevance of this statement is highly obscure at this stage and further studies are highly desirable to clarify the physical nature of the transition and the physical origin for the absence of the hysteresis.

ACKNOWLEDGMENTS

We are grateful for U. Olsson for kindly providing the phase diagram of a $C_{10}E_3$/water system. This work was partly supported by a Grand-in-Aid for Scientific Research from the Ministry of Education, Culture, Sports, Science, and Technology, Japan.

[1] See, for review, e.g., A. Onuki, J. Phys.: Condens. Matter **9**, 6119 (1997).
[2] O. Diat, D. Roux, and F. Nallet, J. Phys. II **3**, 9 (1993); *ibid.* **3**, 1427 (1993).
[3] J. Bergenholtz and N. J. Wagner, Langmuir **12**, 3122 (1996).
[4] J. Zipfel, J. Berghausen, P. Lindner, and W. Richtering, J. Phys. Chem. B **103**, 2841 (1999).
[5] A. Leon, D. Bonn, J. Meunier, A. Al-Kahwaji, O. Greffier, and H. Kellay, Phys. Rev. Lett. **84**, 1335 (2000).
[6] A. Alkahwaji and H. Kellay, Phys. Rev. Lett. **84**, 3073 (2000).
[7] T. D. Le, U. Olsson, K. Mortensen, J. Zipfel, and W. Richtering, Langmuir **17**, 999 (2001).
[8] L. Courbin, J. P. Delville, J. Rouch, and P. Panizza, Europhys. Lett. **55**, 880 (2001); Phys. Rev. Lett. **89**, 148305 (2002).
[9] T. Kato, K. Minewaki, Y. Kawabata, M. Imai, and Y. Takahashi, Langmuir **20**, 3504 (2004).
[10] M. E. Cates and S. T. Milner, Phys. Rev. Lett. **62**, 1856 (1989).
[11] R. Bruinsma and Y. Rabin, Phys. Rev. A **45**, 994 (1992).
[12] S. Ramaswamy, Phys. Rev. Lett. **69**, 112 (1992).
[13] A. G. Zilman and R. Granek, Eur. Phys. J. B **11**, 593 (1999).
[14] S. W. Marlow and P. D. Olmsted, Eur. Phys. J. E **8**, 485 (2002); Phys. Rev. E **66**, 061706 (2002).
[15] S. Brazovskii, Sov. Phys. JETP **41**, 85 (1975).
[16] C. R. Safinya, E. B. Sirota, and R. J. Plano, Phys. Rev. Lett. **66**, 1986 (1991).
[17] K. A. Koppi, M. Tirrell, and F. S. Bates, Phys. Rev. Lett. **70**, 1449 (1993).
[18] H. F. Mahjoub, K. M. McGrath, and M. Kleman, Langmuir **12**, 3131 (1996); H. F. Mahjoub, C. Bourgaux, P. Sergot, and M. Kleman, Phys. Rev. Lett. **81**, 2076 (1998).
[19] J. Yamamoto and H. Tanaka, Phys. Rev. Lett. **77**, 4390 (1996).
[20] A. Leon, D. Bonn, J. Meunier, A. Al-Kahwaji, and H. Kellay, Phys. Rev. Lett. **86**, 938 (2001); A. Leon, D. Bonn, and J. Meunier, J. Phys.: Condens. Matter **14**, 4785 (2002).
[21] L. Porcar, W. A. Hamilton, P. D. Butler, and G. G. Warr, Phys. Rev. Lett. **89**, 168301 (2002); L. Porcar, W. A. Hamilton, and P. D. Butler, Langmuir **19**, 10779 (2003).
[22] P. Panizza, L. Courbin, G. Cristobal, J. Rouch, and T. Narayanan, Physica A **322**, 38 (2003).
[23] D. A. Huse and S. Leibler, J. Phys. (France) **49**, 605 (1988).
[24] G. Porte, J. Phys.: Condens. Matter **4**, 8649 (1992).
[25] J. Yamamoto and H. Tanaka, Phys. Rev. Lett. **74**, 932 (1995).
[26] J. Yamamoto and H. Tanaka, Nat. Mater. **4**, 75 (2005).
[27] P. D. Butler, L. Porcar, W. A. Hamilton, and G. G. Warr, Phys. Rev. Lett. **88**, 059601 (2002); H. F. Mahjoub, C. Bourgaux, J. F. Tassin, and M. Kleman, Phys. Rev. Lett. **88**, 059602 (2002).
[28] P. Snabre and G. Porte, Europhys. Lett. **13**, 641 (1990).
[29] O. Diat and D. Roux, Langmuir **11**, 1392 (1995).
[30] G. Porte *et al.*, J. Phys. II (France) **1**, 1101 (1991).
[31] S. T. Milner, M. E. Cates, and D. Roux, J. Phys. (France) **51**, 2629 (1990).
[32] L. Porcar, W. A. Hamilton, P. D. Butler, and G. G. Warr, Phys. Rev. Lett. **93**, 198301 (2004).
[33] A. G. Zilman and R. Granek, Phys. Rev. Lett. **77**, 4788 (1996).
[34] See, e.g., H. Tanaka, J. Phys. Soc. Jpn. **69**, 299 (2000).
[35] G. Porte, J. Apell, P. Bassereau, and J. Marignan, J. Phys. (France) **50**, 1335 (1989).
[36] L. Porcar, G. G. Warr, W. A. Hamilton, and P. D. Butler, Phys. Rev. Lett. **95**, 078302 (2005).